Sensors & Actuators: B. Chemical 291 (2019) 58–66

Contents lists available at ScienceDirect

Sensors and Actuators B: Chemical

journal homepage: www.elsevier.com/locate/snb

Rapid isolation of *Escherichia coli* from water samples using magnetic microdiscs

Keisha Y. Castillo-Torres[a], David P. Arnold[a,*], Eric S. McLamore[b]

[a] Electrical and Computer Engineering Department, Interdisciplinary Microsystems Group, University of Florida, Gainesville, FL 32611, United States
[b] Agricultural and Biological Engineering Department, Institute of Food and Agricultural Sciences, University of Florida, Gainesville, FL 32611, United States

ARTICLE INFO

Keywords:
Bacteria detection
Magnetic isolation
Viability staining
Irrigation/drinking water analysis

ABSTRACT

This work introduces a method for rapid isolation of target bacterial cells using "bacteria-sized," gold-coated magnetic microdiscs (1.5 μm in diameter, 80 nm in thickness). These microdiscs are functionalized with DNA aptamers for selectively isolating *Escherichia coli* cells from lab-prepared and environmental water samples at concentrations as low as 10^2 CFU/100 mL with no enrichment. This microdisc platform enables viability assay on the magnetically captured discs using fluorescent markers such as SYTO9, propidium iodide, and carbon quantum dots, providing both a detection and viability step in a single analysis. The significance of this gravity-driven separation technique is the ability to rapidly isolate target cells from relatively large sample volumes (up to 100 mL) with simple field-deployable apparatus in one step, without the use of complicated equipment or energy. This technique has immediate application for rapid (< 45 min) isolation and detection of fecal indicators (*E. coli*) in agricultural water and can be used for drinking water analysis if an enrichment step is added. In addition to targeting *E. coli*, the platform can be used for targeting other cells based on functionalization of the microdiscs with other bioreceptors such as aptamers, lectins, phages, or peptides.

1. Introduction

Globally, more than 900,000 deaths are reported every year related to foodborne and waterborne diseases [1,2]. Ensuring safe food and water represents a global concern and an ongoing societal challenge, and one of the primary sources of contamination is fecal material from animals. Dating back to the World Health Organization guidelines of 2006 [3], most regulations for food and water are based on a tolerable additional disease burden of 10^{-6} DALYs (disability adjusted life years) per person per year (pppy). This risk-based approach does not consider the number of pathogens in a given volume, but rather how many viable pathogens can be ingested without exceeding the tolerable disease burden at the population scale. In the US, the current regulatory framework is based on sample volumes of 100 mL for both fresh produce and drinking water. This relatively large sample volume is critical to ensure that adequate sample size produces statistically meaningful data regarding change(s) in tolerable disease burden.

For drinking water, the U.S. Environmental Protection Agency (EPA) standards and regulations require presence of less than 10^0 CFU/100 mL, and rapid detection is a priority so critical management steps can be implemented to alleviate the problem and maintain DALYs less than 10^{-6} pppy [4]. The emerging paradigm for ensuring safe drinking water in distribution systems is based on the framework of smart water networks [5], where sensors provide rapid feedback to managers for improving decision support and limiting risk. For smart water networks to be a reality, a portfolio of portable, rapid, and low-cost testing systems are highly needed. Standard culture-based methods are accurate and will remain a useful tool for the foreseeable future, but these techniques are labor intensive, laboratory based, and require up to one day for results. Emerging methods such as nucleotide-based sensors, polymerase chain reaction, and immunoassays have demonstrated low concentration detection limits for *E. coli* (10^3–10^5 CFU/100 mL) for water/food samples [6,7] but are limited to low sample volumes of 1–10 mL, require complex lab tools/equipment, need trained expert users, and require test times of 1–24 h [7].

Among the plethora of sensors for detecting *E. coli* in drinking water (reviewed by [8]) sensors based on aptamers have proven to be highly efficient. Aptamers are durable, can be mass produced without the need of animal housing processes, and the binding affinity and sensor performance are comparable, or superior to, antibodies used in immunoassays. A variety of platforms have been used for creating *E. coli* sensors and among these, methods that employ magnetic structures are gaining attention. The recent focus on magnetic biosensor platforms is due to the material biocompatibility and also the unique ability to non-

* Corresponding author.
E-mail address: darnold@ufl.edu (D.P. Arnold).

https://doi.org/10.1016/j.snb.2019.04.043
Received 9 January 2019; Received in revised form 12 February 2019; Accepted 8 April 2019
Available online 10 April 2019

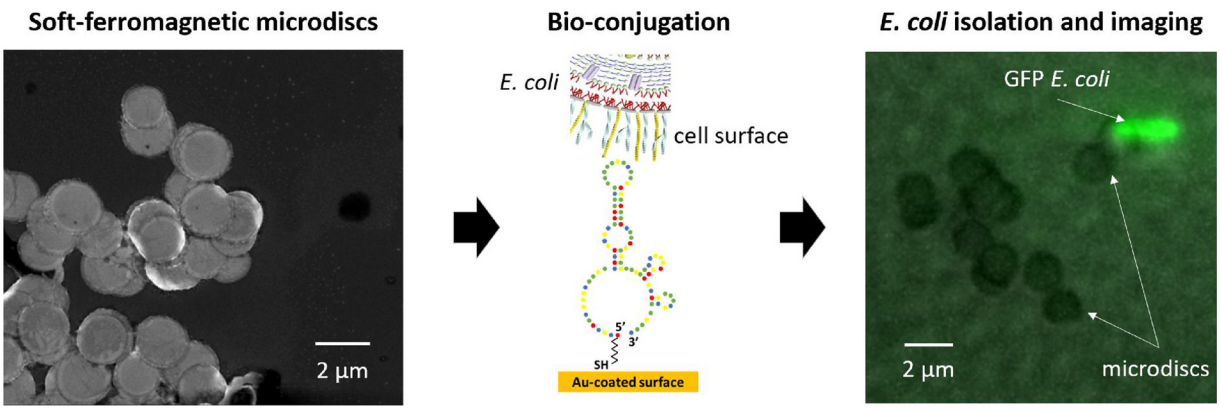

Scheme 1. Overall concept (from left to right) 1) SEM image of magnetic microdiscs, 2) concept of surface bioconjugation using thiolated aptamers, 3) and fluorescent microscope image showing isolation of GFP *E. coli* from a water sample.

invasively actuate and/or interrogate the sample using external magnetic fields [9–11].

Magnetic nanoparticles (MNPs) have been used for magnetic imaging contrast enhancement agents, magnetic hyperthermia, drug delivery, and magnetic separation of cells [9–12]. A key feature of MNPs is their superparamagnetic behavior (ideally zero magnetic remanence), which inhibits inter-particle magnetic dipole interactions and thus unwanted magnetic agglomeration of particles when in suspension [11]. However, for a magnetic particle to exhibit superparamagnetic behavior, the particle diameter is limited to a few tens of nanometers. For example, the ubiquitously used superparamagnetic iron oxide nanoparticles (SPIONs) are superparamagnetic up to only ~20 nm, above which the particles are considered magnetically blocked and hence retain a small dipole moment even in the absence of a magnetic field. Upon application of a field, the SPIONs are typically driven to magnetic saturation with a saturation magnetization of typically $\mu_0 M_s = 0.58$ T (90 emu/g) [13–16]. Because the net magnetic moment of a single ~20-nanometer particle is too small for many applications, the MNPs are often mixed with polymers (e.g. polystyrene) and used to form larger micron-sized magnetic beads. However, the magnetic volume fraction can be up to 70% [17], which means the effective saturation magnetization of a single bead is only 0.41 T. MNPs have been used to magnetically isolate *E. coli*, among other cells but detection limits (10^3–10^9 CFU/100 mL) have not reached levels relevant to drinking water quality monitoring set by the EPA. [11,18–21].

An alternative to MNPs for biomagnetic applications is the use of metal or metal alloy (typically $Ni_{80}Fe_{20}$) "spin-vortex" discs. A spin-vortex disc is a disc-shaped nanostructure, that under the right dimensions, exhibits a self-enclosing vortex arrangement of the atomic moments in the absence of a magnetic field [22,23]. Like a SPION, these discs are characterized by near-zero remanence (see supplemental Fig. S–1A), but much higher saturation magnetization, $\mu_0 M_s = 1.00 \pm 0.01$ T (91.16 ± 1.34 emu/g). The magnetic microdiscs (1.5 µm in diameter, 80 nm in thickness) are lithographically patterned, which provides reliable control of size, shape, structure, and function. Furthermore, the magnetic microdiscs are already micron-sized and fully magnetic. The saturation magnetic moment of one disc is up to 6 orders of magnitude larger compared to typical SPIONs (~200,000 times larger than typical magnetic beads), and therefore these particles can impart much higher magnetic forces and/or make use of smaller magnetic fields and field gradients. Another distinguishing advantage is that the magnetic discs can impose torques, whereas SPIONs and magnetic beads cannot.

All these advantages make magnetic microdiscs of interest for bioapplications, especially for (micron-sized) cell targeting and magnetic isolation. For example, use of these discs have been explored and demonstrated to target and trigger cancer cell apoptosis and magnetic hyperthermia by introducing an alternating magnetic field that creates a rotating magneto-mechanical stimulus on the discs and therefore on the cells [12,24]. Similarly, previous works on these discs have demonstrated the ability to characterize fluidic sample properties (i.e. viscosity) by also actuating the discs with a rotating magnetic field [25]. Our group has also reported preliminary results for selective targeting and isolation of bacteria using these discs as well [26,27].

This work aims to extend the study on bacteria targeting using surface-functionalized gold-coated magnetic microdiscs to detect presence and viability of *Escherichia coli* in irrigation/drinking water and other complex matrices samples. Herein, we show *E. coli* isolation using DNA aptamer-functionalized magnetic microdiscs at detection levels of down to 10^2 CFU/100 mL (79% of infectious dose for irrigation water, FDA FSMA) in less than an hour using three different fluorescent tags for imaging: green fluorescent protein (GFP), SYTO9/propidium iodide (PI), and carbon quantum dots (CDs).

A long-term goal of this method is to develop a water monitoring system that serves as a rapid indicator of presence of fecal material in water samples. Once the detection of *E. coli* is performed, the water sample can be subject to analysis under a more specific biosensor. The significance of our technique is that it provides a platform for rapid screening for bacteria with limits of detection reaching as low as 10^2 CFU/100 mL using simple fluorescent imaging. The total protocol requires less than 45 min for non-enriched samples, and if combined with rotational stimulus of discs to enhance bacteria binding and a smartphone imaging platform, one can envision a rapid, portable bacteriological screening tool.

Scheme 1 shows the concept of our microfabricated magnetic microdiscs, their surface functionalization, and bacteria isolation from water samples. In summary, DNA aptamers are used as the capture probes to functionalize our gold-coated magnetic microdiscs to isolate *E. coli* from water samples and detect presence and viability of *E. coli* using different fluorescent labels (i.e. GFP, SYTO9/PI, and CDs).

In our previous work [26,27], we showed preliminary results of a similar strategy using a thiolated 39-mer specific to O-antigen on *E. coli*. using DNA aptamers. In this work, we expand the study by using an aptamer specific to ATCC 25922 and investigate the role of base pair mismatches within the stem loop structure, as well as increasing the sample volume to meet field testing requirements.

2. Materials and methods

See supplemental section for chemicals and reagents.

2.1. Bacteria enumeration and fluorescent labeling

Lyophilized *E. coli* pellets (ATCC 25922; FDA strain 1946) were equilibrated at room temperature for 30 min while the hydrating buffer was warmed to 34 °C per the protocol from the manufacturer. See

supplemental section for details on preparation of bacteria suspensions, including live and dead cell preparations. Where noted, mixtures of viable/non-viable cells were obtained following the protocol in the BacLight LIVE/DEAD kit.

Three different approaches were used for cell imaging, namely: i) SYTO9/PI labeling, ii) CD viability staining, or iii) GFP transformation. SYTO9/PI staining was conducted following the protocol in the BacLight kit. An aliquot (3 μL) of SYTO9 was mixed with 3 μL of 20 mM PI and 1 mL of bacterial suspension. This solution was maintained at room temperature for 15 min and then washed 3 times using phosphate buffer saline (PBS) buffer. For CD labeling of viable cells, the methods reported by Liu et al. [28] were used. Briefly, *E. coli* cells were grown in TSB at 37 °C for 6 h, diluted, and then washed in PBS buffer. A cell suspension (1 mL) was mixed with an aliquot of CD (75 μL) and vortex mixed. The mixture was incubated on a shaker table (30 rpm) at 37 °C for 6 h. Samples were then added to disc solutions for confocal microscopy as described below. GFP transformed cells provided by EnCor Biologics, Inc. were grown in TSB at 37 °C for 6 h, diluted, and then washed in PBS buffer.

During initial studies, positive control samples were collected from a local municipal wastewater treatment plant in Gainesville, FL (UF Water Reclamation Facility). Samples were collected from the effluent wier of the secondary clarifier and analyzed on the same day of collection.

2.2. Microfabrication of gold-coated magnetic microdiscs

The magnetic microdiscs were microfabricated using standard microfabrication techniques. A densely packed array of circular polymer pillars (1.5 μm in diameter) were formed on a 100-mm-diameter silicon substrate similar to [26,27]. Cleaning process of (100) p-type Silicon test wafers consisted of separate submersion steps in positive resist stripper 3000 (PRS3000) and buffered oxide etching (BOE), followed by some rinsing, drying, and/or de-hydration steps. Then, a 100-nm layer of tungsten was deposited as a sacrificial layer, at a deposition rate of 0.1 nm/s, using magnetron sputtering (Kurt J. Lesker multi-source RF and DC sputter system) followed by spin-coating a 300-nm thick layer of lift-off resist (LOR 3 A) and 800-nm thick layer of a positive photoresist (AZ 1512). Polymer resists (LOR and AZ 1512) were patterned by standard UV exposure (vacuum contact) and developed (AZ300MIF) for 1 min, forming a lift-off masking layer. Then, gold and permalloy ($Ni_{80}Fe_{20}$) metals were deposited by magnetron sputtering followed by an ultra-sonicated lift-off process to obtain the permalloy magnetic microdisc array using AZ400 K diluted in water (1:4). Finally, the microdiscs were released by dissolving the tungsten sacrificial layer using 30% hydrogen peroxide and rinsed three times with DI water using a permanent magnet to decant supernatant. Scheme 1a represents an image of dried magnetic microdiscs on a silicon substrate. Refer to supplemental Fig. S–1B for more detail on the microfabrication process of the microdiscs.

2.3. Bio-conjugation of aptamers to gold

An 88-mer aptamer (P12-55; MW = 11.8 kDa; K_D = 0.83 nM) that specifically binds to *E. coli* 25922 cells [29] was synthesized by GeneLink, Inc. (Hawthorne, NY, USA). A scrambled version of the P12-55 aptamer with three single basepair (bp) mismatches was also tested. One bp scramble was positioned within the main stem loop (T–G replacement), and the other two bp scrambles were in the apical stem loop (G–T replacement); see supplemental Fig. S–2 for details and sequences. All aptamers were thiol-terminated at the 5′ end with a C6 spacer bound to the C residue for covalent binding to gold-coated surfaces. See supplemental Fig. S–2 for additional information.

Aptamers were conjugated to gold electrodes following the methods in Burrs et al. [30] and Rong et al. [31]. An aliquot of 1–5 million discs were suspended in 200–300 μL of the aptamer buffer solution and stored overnight at room temperature. After overnight storage, discs were rinsed three times with DI water using a permanent magnet to decant supernatant and then microdiscs were biofunctionalized with aptamers (after de-protecting the thiol tag following the protocol by GeneLink). Briefly, a disposable microwell was fixed to the electrode and the de-protected aptamer was drop cast into the well, then allowed to bind for 6 h. The microwell fixture was subsequently removed and the surface rinsed three times in DI prior to analysis.

2.4. E. coli sample preparation and imaging on microdiscs

E. coli 25922 stock concentration used for experiments consisted of 10^4 CFU/100 mL. See supplemental section for details on the sample preparations for the three kinds of fluorescent assays (SYTO9/PI, CD live cell tagging, and GFP transformed cell imaging). In summary, SYTO9/PI staining was conducted following the protocol in the BacLight kit (3 μL of SYTO9; 3 μL of 20 mM PI; 1 mL of bacterial suspension). CDs were produced following the methods by Sun et al. [32], with slight modification. These CDs with quantum yields ranging from 4 to 10% in response to an excitation of 400 nm [32], possess tunable fluorescent properties, low-cost, and low-environmental toxicity when compared with other live/dead stains [32–35]. All GFP *E. coli* were grown to a concentration of 10^{11} CFU/100 mL and diluted prior to imaging as noted.

Cells were incubated with the magnetic microdiscs for 15–20 min at room temperature, rinsed with PBS buffer, tagged with SYTO9/PI and rinsed with PBS buffer again. Rinsing steps were done by magnetically concentrating the microdiscs with a permanent magnet, decanting supernatant and re-suspending in new buffer. The magnetic microdiscs bound/unbound to target cells (viable and/or non-viable) were rinsed as described above, magnetically concentrated and retrieved from the vial using a 10 μL pipette and deposited on a glass slide for fluorescent or confocal microscopic imaging and inspection. For imaging of CD-labeled cells, *E. coli* that had been previously incubated with CD solutions (as described in section 2.3) were exposed to 2 million discs, captured with a single permanent magnet, and then transferred to a glass slide for imaging. GFP *E. coli* (10^8 CFU) were exposed to 2 million magnetic microdiscs and incubated for 20 min, captured with a permanent magnet, and imaged.

2.5. Confirmation of E. coli binding using electrochemical testing

Prior to testing aptamer-functionalized microdiscs, aptamer binding to *E. coli* 25922 was verified using standard electrochemical impedance spectroscopy (EIS) as described by Hills et al. [36]. EIS tests were performed in 4 mM potassium K_4FeCNH_6 and 1 M KCl at 20 °C. An initial DC voltage of 0.25 V and an AC voltage of 100 mV with a frequency range of 1 Hz to 100 kHz were applied and used for all tests.

3. Results and discussion

3.1. Affinity of thiolated aptamer for E. coli

Prior to testing aptamer-functionalized microdiscs, a commercial gold disc electrode (1.6 mm diameter) was used to confirm *E. coli* 25922 binding for the primary aptamer (P12-55) and for the scrambled aptamer. Bode plots (Fig. 1A) show an increase in impedance during stepwise addition of *E. coli* using aptamer P12-55 88mer. The response was linear across the range of 10^1 to 10^6 CFU/100 mL at a cutoff frequency of 6.31 Hz using Faradaic impedance with 4 mM K_4FeCN_6 as the redox probe. Fig. 1B shows a that cutoff frequency was optimal at 6.31 Hz based on linear regression coefficient (calibration curves) and sensitivity toward *E. coli*. This data clearly show that aptamer P12-55 is selective for *E. coli* 25922, and that the functionality is directly correlated to the sequence selected from the SELEX process by Marton et al [29]. Although the specific molecular target of aptamer P12-55 was not

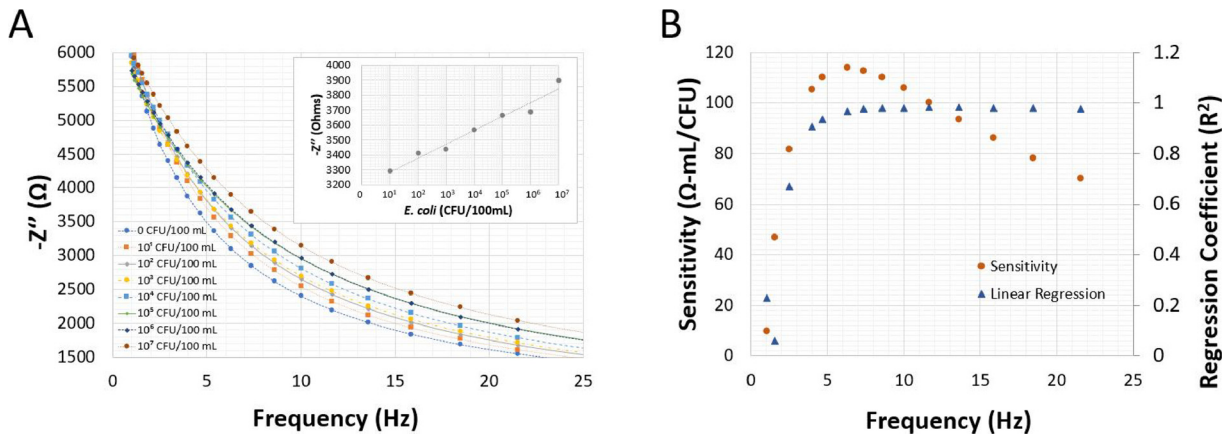

Fig. 1. Electrochemical impedance spectroscopy analysis of thiolated aptamers on a gold electrode toward *E. coli* 25922. (A) Bode plots for P12-55 88mer; inset shows linear calibration plot using impedance at a cutoff frequency of 6.31 Hz (Faradaic impedance with 4 mM K_4FeCN_6) (B) Cutoff frequency was performed between 1–21.54 Hz for sensitivity toward *E. coli* and linear regression coefficient.

reported by Marton et al. [29], the authors estimate that the aptamer has a high affinity for *E. coli* 25922 cells, with an estimated 14,950 binding sites on a single *E. coli* cell. On the other hand, the scrambled aptamer (three single bp substitutions in the stem-loop structures) did not respond to *E. coli* 25922 at any concentration (see supplemental section). This result confirms the results by Marton et al. [29] in studies of aptamer-cell suspensions and validates that single bp substitutions to the stem-loop region significantly alter binding affinity, likely resulting from a change in secondary structure.

To further challenge this result, the specificity of aptamer P12-55 and the scrambled aptamer were tested with other Gram negative cells and the aptamer was at least 92% selective over all other cells tested. (See Supplemental Fig. S–2C)

3.2. Isolation of viable and non-viable E. coli using bio-conjugated magnetic microdiscs

Microdiscs with P12-55 aptamer (40 nM/mm^2) demonstrated successful capture of *E. coli* 25922 from 100 mL samples. To further extend this result, viability was assessed using common staining methods: i) live/dead staining by SYTO9/PI, and ii) CD staining of live cells, as well as GFP transformed cells (positive control). Refer to Fig. S–8 for schematic of approach and details of methods. Fig. 2 shows representative confocal images (bright and fluorescent fields) of aptamer-functionalized magnetic microdiscs exposed to SYTO9/PI-stained *E. coli* 25922 samples. The concentration after incubation was 10^4 CFU/100 mL (Fig. 2A), 10^2 CFU/100 mL (Fig. 2B), 10^0 CFU/100 mL (Fig. 2C), and 0 CFU/100 mL (control) (Fig. 2D). As shown in the images, the fluorescence signal is directly correlated to bacteria concentration, and no signal is apparent in control samples, which validates the utility of our approach for *E. coli* detection. Due to the stacking and agglomeration of discs during the capture process, it is currently not possible to provide quantitative cell counts, although the capture mechanism is highly useful for rapid screening and disc actuation methods (i.e., spin vortex) are possible in future studies, which is discussed in a later section. Consistent with other fluorescent viability assays, the test shown in Fig. 2 is limited by the accuracy of the fluorescent label for reporting cell viability. Given the known promiscuity of SYTO9 for staining extracellular DNA, or eDNA [37], it is possible that the green rod-like features in Fig. 2 are cell debris, and not viable cells as reported by many previous manuscripts. To further explore the use of micron-sized discs as capture probes, alternative fluorescent labels were compared during simulated field testing as discussed in section 3.3.

3.3. Fluorescence labeling of isolated E. coli in water samples

To determine the broad applicability of the technique, a comparative study was conducted using three fluorescent techniques, namely: GFP transformed cells, CD-labeled viable cells, and SYTO9/PI stained cells. Fig. 3 shows representative fluorescent images after *E. coli* 25922 capture using aptamer-functionalized magnetic microdiscs. GFP-transformed *E. coli* (Fig. 3A) are visible along the edges of the discs, and the rod-like structure is apparent with little debris or artifact, indicating successful capture by the aptamer-coated microdiscs. Likewise, CD-labeled *E. coli* (Fig. 3B) capture is apparent based on the morphologically appropriate rod structures near discs and lack of significant debris. The relatively low level of debris is attributed to the uptake of CD by viable cells as compared to the non-specific staining that is common to other labeling techniques. SYTO9/PI-tagged *E. coli* (Fig. 3C) are visible, but there was significant debris and artifact in all samples, which is a common problem in SYTO9 staining as any eDNA would be labeled by SYTO9. There was some visible PI (red channel) in the samples shown in Fig. 3C, but the high uncertainty regarding false positives was deemed unacceptable for water quality testing. Given the false positive issue common to SYTO9 staining, as well as the low shelf life of the stain, CD-labeling was selected as the most viable option for development of a rapid viability biosensor in further testing among the methods tested herein. Thus, this approach was challenged in water samples and compared to literature values.

3.4. E. coli 25922 detection in water samples and comparison to literature detection in water samples and comparison to literature

Fig. 4 depicts the overall process of the testing protocol for samples of up to 100 mL. The technique is simple, utilizes readily available, low-cost items (glass funnel, beaker, neodymium magnets), and can interface with any fluorescent detection system that is capable of imaging bacterial targets and/or other downstream biosensors. *E. coli* 25922 detection was demonstrated using aptamer-functionalized microdiscs in sample volumes ranging from 0.5 mL to 100 mL, and bacteria concentrations ranging from 10^0 to 10^{11} CFU/100 mL. Samples with *E. coli* concentrations above 10^2 CFU/100 mL were analyzed within less than 45 min (Figs. 2–3). However, dilute samples below this threshold (e.g., 10^0 CFU/100 mL) required enrichment for accurate detection (Fig. S–7). For screening dilute samples, the solution was incubated with TSB for 6 h at 37 °C. For screening concentrated solutions, no enrichment is required as shown in Figs. 2–3. For application in drinking water within the US, an enrichment step is required since the maximum containment level goals for *E. coli* are zero in 40 samples per month according to the revised total coliform rule [38]. For screening watersheds, or targeting

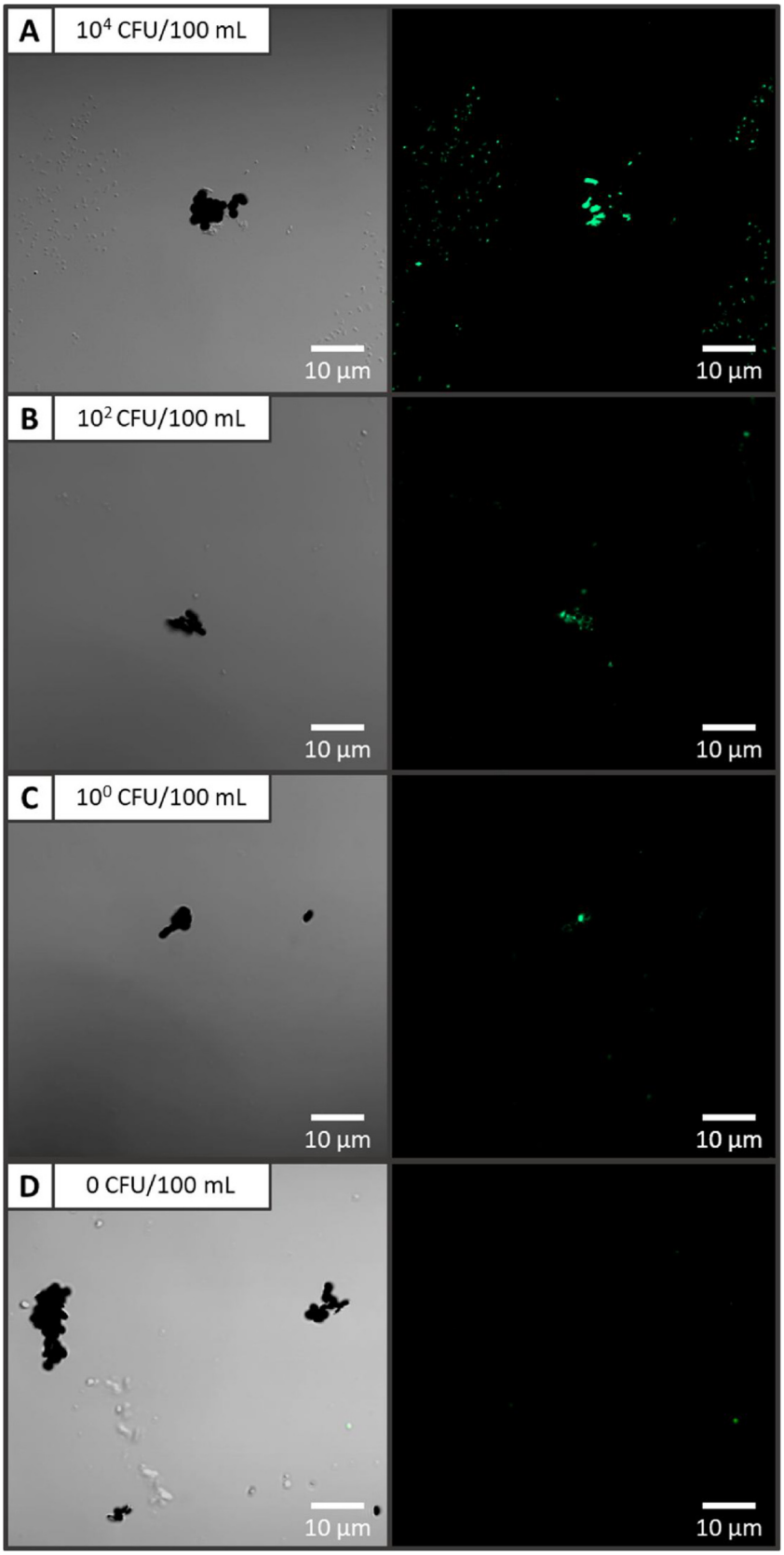

Fig. 2. Example (bright and fluorescent fields) images of samples containing aptamer-functionalized discs exposed to viable *E. coli*A) 10^4 CFU/100 mL, B) 10^2 CFU/100 mL, C) 10^0 CFU/100 mL, and D) 0 CFU/100 mL no cells (control). All samples were tagged using SYTO9/PI.

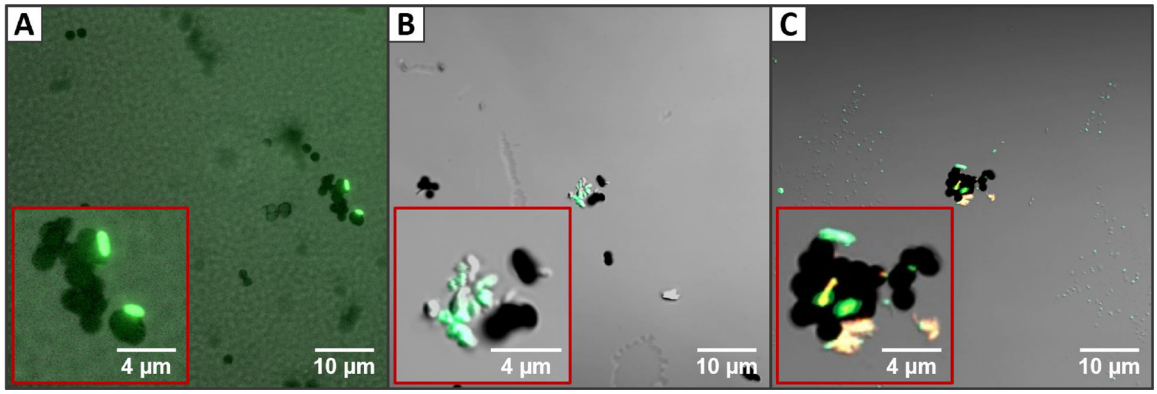

Fig. 3. Fluorescence labeling of *E. coli* 25922 was demonstrated using three different approaches: A) green-fluorescence protein (GFP) transformation, B) carbon dot (CD) labeling, and C) SYTO9/propidium iodide (PI) staining. (For interpretation of the references to colour in this figure legend, the reader is referred to the web version of this article).

other pathogenic bacteria, the technique has applications where direct use is possible (e.g., in studies screening for pathogens with a high infectious dose in the range of 10^3 to 10^8 cells, such as *Vibrio cholera*; [39]).

To demonstrate the versatility of the method using other receptors, various capture probes were also tested (for an example of microdiscs coated with the lectin ConA, see supplemental Fig. S–7). In agricultural applications (e.g., irrigation water screening), the current food safety modernization act (FSMA) guidelines require that a minimum of 20 water samples have less than 126 CFU/100 mL, and samples must be processed within 8 h of collection [40]. For these levels and timeframe, the microdisc method is directly applicable by using the enrichment step, although further studies are needed to investigate the minimum enrichment time and temperature required for detection of dilute *E. coli* samples in various water samples.

Performance characteristics of the microdisc capture method was compared to different methods using magnetic particles as summarized in Table 1. The limit of detection (LOD) reported in the literature ranges from 3.0×10^0 to 1.5×10^9 CFU/100 mL, while response times ranged between 0.35–2.5 h. The microdisc method herein demonstrated *E. coli* detection using aptamer-functionalized discs in samples of 0.5–100 mL and bacteria concentrations as low as 10^2 CFU/100 mL in less than an hour. However, preliminary results (supplemental Figs. S–7C and S–7D) have been obtained on samples of up to 100 mL and *E. coli* concentrations down to 10^0 CFU/100 mL within 8 h. Using our microdisc capture method, the LOD for non-enriched samples (10^2 CFU/100 mL) is within the same range, and the response time is less than one hour. Obtaining LOD values down to 1 CFU/100 mL using the microdisc platform is possible with sample enrichment, in which case the response time is 8 h for a concentration of 1 CFU/100 mL. While this magnetic microdisc method requires enrichment to meet EPA thresholds in drinking water (1 CFU/100 mL in less than 8 h), the technique is directly applicable for detection of fecal coliforms in irrigation water (126 CFU/100 mL in less than an hour). Havelaar et al. [40] recently analyzed six agricultural irrigation ponds and found that the current FSMA rule grossly underestimates true pathogen levels and the sampling strategy is not

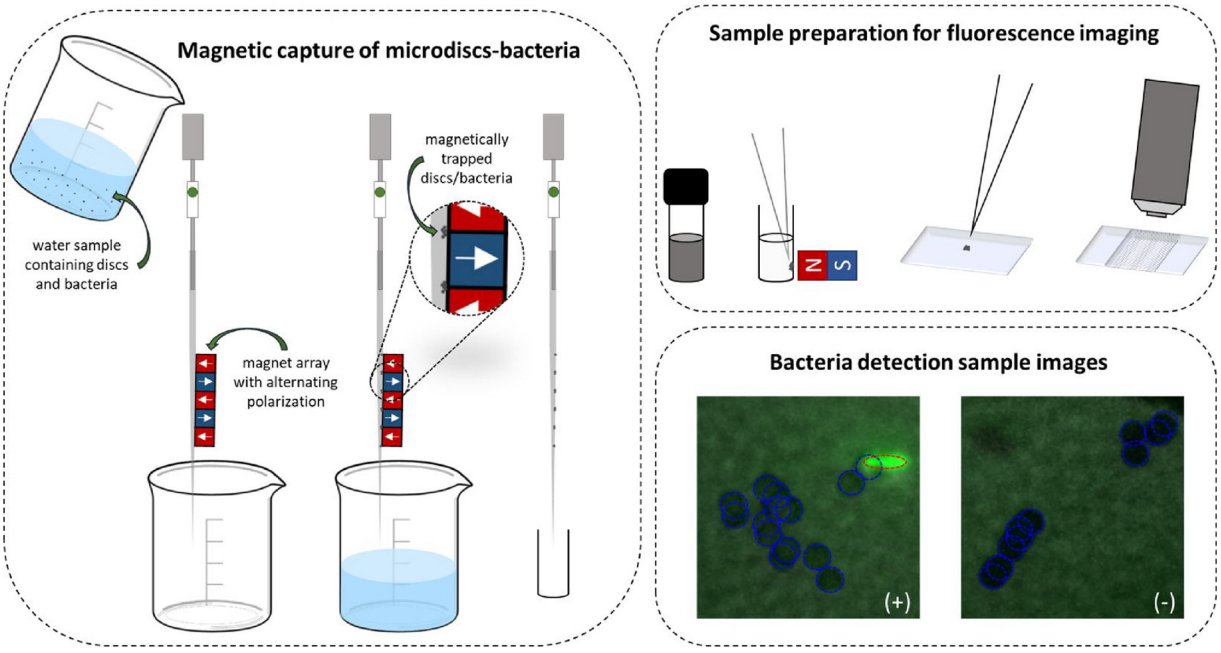

Fig. 4. (left) Magnetic capture procedure and representative image. This procedure uses a fluidic channel built with a glass pipette and an array of magnets with alternating polarization to increase high magnetic gradient contact points with the sample. (top right) For imaging, discs are subsequently collected using a single permanent magnet. (bottom right) Image acquisition can be performed with an epi-fluorescence scope, confocal scope, or other envisioned device such as a smartphone based fluorescence scope. In sample images, blue circles depict magnetic microdiscs while red oval depicts*E. coli* (For interpretation of the references to colour in this figure legend, the reader is referred to the web version of this article).

Table 1
Biosensing characteristics of *E. coli* detection methods using magnetic particles.

Method	Magnetic particles (material and size)	Selectivity (capture probe)	Sample volume (mL)	Limit of detection (CFU/100 mL)	Response time (hr)	Viability step?	Ref
Impedance biosensor coupled with MNP-antibodies	Streptavidin-coated Fe_3O_4 NPs (145 nm)	biotin-labeled polyclonal goat antibodies (*E. coli*)	0.5	7.4×10^6	0.58	No	[20]
Immunomagnetic separation (IMS) and electrochemical (EC) detection	Polyaniline-coated gamma iron oxide NPs (20 nm-unmodified, 50–100 nm-coated)	Monoclonal anti-*E. coli* O157:H7 antibodies	0.1	6.0×10^2	1.08	No	[41]
IMS and EC detection	Magnetic beads (Dynabeads MAX) and polystyrene secondary beads (2.8 μm)	*E. coli* O157:H7 antibody	1–100	3.0×10^0	2.00	No	[42]
Bacteria magnetic capture and disinfection	Fe_3O_4 NPs synthesized with CTAB (10 nm)	Cetyltrimethyl-ammonium bromide (CTAB)	5.0	1.5×10^9	1.00	No	[43]
Bacteria removal using magnetic graphene composite and MNPs	Fe_3O_4 / graphene composite NPs synthesized and Fe_3O_4 NPs (10 nm-unmodified, 15–25 nm-composite)	Solvothermal synthesis	1–2.05	1.0×10^4	> 0.50	Yes	[44]
Magnetophoretic chromatography and colorimetric detection using MNPs	Platinum-coated Fe_3O_4 clusters (150 nm)	half-fragments of *E. coli* antibodies	10 (milk)	1.0×10^3	0.50	No	[19]
Electrochemical immunosensor using antibody-functionalized MNPs	Polyaniline-coated γ -Fe_2O_3 NPs (50–100 nm)	monoclonal antibodies	0.5	1.0×10^3	< 1.00	No	[21]
Nuclear magnetic resonance	gamma iron oxide NPs (50–100 nm)	*E. coli* O157:H7 antibody	0.1	7.6×10^2	0.35-0.52	No	[45]
MTT (colorimetric) assay using MNPs	Cobalt ferrite NPs 7 nm	amine-functionalized MNPs	5.0	1.5×10^9	1.00	No	[46]
Magnetic reduced graphene oxide (rGO) nanoheaters for selective isolation of *E. coli*	magnetic particles (MPs) anchored on rGO nanocomposites	2-nitrodopamine modified MPs	10	1.0×10^3	0.50	Yes	[47]
Bacterial capture and detection using aptamer—based hydrogel magnetic barcodes	Poly (ethylene glycol) hydrogel inverse opal particles (~150 nm)	aptamer-functionalized barcodes	0.1	1.0×10^4	2.50	No	[48]
Magnetic isolation using spin-vortex magnetic microdiscs + fluorescent assay	Permalloy microdiscs (Ø: 1.5 μm, thickness: 80 nm)	DNA aptamers	0.5–100	1.0×10^2-1.0×10^3	< 0.50	Yes	This work

sufficient for indicating microbial contamination until several years of data are collected. Havelaar et al. suggest a more targeted risk management strategy based on comprehensive and frequent analysis of water quality parameters to inform preventive or rapid corrective actions, particularly during peak contamination events. Therefore, the method herein presented represents a potential alternative to target and isolate fecal coliforms at detection levels as low as 10^2 CFU/100 mL in less than an hour with the capability of viability detection.

Other than the immunomagnetic separation method by Jayamohan et al. [42] that incorporated commercial magnetic beads, none of the sensors in Table 1 tested sample volumes of up to 100 mL (most sensors tested volumes of 0.1–10 mL) and only one other method [44] included a viability step. Table 1 also shows that most of the magnetic particles used in *E. coli* biosensors consisted of iron oxide particles with diameters raging between 50–150 nm. These MNPs (tens of nanometers) are in many cases coated and/or combined with polymers and/or polysterene NPs (i.e. polyaniline, polystyrene beads, and PEG), which when compared to our magnetic microdiscs (1.5 μm in diameter, 80 nm in thickness), are approximately 236,000 times smaller. While there are known benefits to using nanoscale sensor platforms (higher surface volume to area), there are also major challenges in terms of recovering the material from environmental samples, unknown toxicity at field scale, and unknown fate and transport in the environment. In addition to these issues, details on the MNP assay selectivity to *E. coli* was described in terms of the specific capture probes used for their assays. Here, the microdisc capture method is proposed as a platform solution and a variety of antibodies, amines, aptamers, and other capture probes were presented. Given that the microdisc approach can detect low levels of viable *E. coli* in under one hour, this method is an excellent platform for rapid screening of water samples and can easily target other cells by changing the capture probe.

3.5. Bacterial detection acquisition system and future perspectives

This method provides versatility in terms of the capture probes that can be used (i.e. aptamers, lectins, antibodies, and others), but also in terms of the fluorescent labels that can be used (i.e. different sizes of quantum carbon dots) to identify different kinds of cells (see preliminary results in Fig. S–10). Preliminary results have been obtained using Concavalin A (ConA) lectins as capture probes while targeting coliforms (i.e. *E. coli.*, *K. variicola*, and *P. mirabilis*), see supplemental Figs. S–7C and S–7D. These preliminary results were obtained from, not only lab-prepared water samples but also, from more complex samples (i.e. vegetable broth), see supplemental Figs. S–11 and S–12. The microdisc capture method represents the advantages of being field-ready (when access to portable fluorescence microscope) and detecting viability within 8 h, as well as potentially detecting cell counts as low as 1 CFU/100 mL. While other biosensors, such as impedimetric aptasensors, are accurate and highly useful, these sensors require expensive equipment, trained personnel, and considerable *ad hoc* data analysis for interpreting results. Although outside the scope of this manuscript, it is envisioned that combining this bacteriological screening method with rotational stimulus of microdiscs could enhance bacteria binding and provide a unique actuation step to the capture process shown here, potentially paving new roads for microdiscs which follow the sense-analyze-respond paradigm. There is an opportunity to combine this simple method with smartphone-based imaging platforms [49], machine vision classifiers [50], and data analytics [31] for providing rapid, portable detection of fecal indicators in water samples.

4. Conclusions

Rapid detection of *E. coli* in drinking water is vital to ensuring the safety of the public, and without sensing capabilities, smart water networks such as those proposed by Rasekh (2016) are not possible. This work demonstrated the ability to rapidly (< 45 min) isolate *E. coli* from water samples at levels of 10^2 CFU/100 mL using bio-conjugated (i.e. aptamer) magnetic microdiscs. Also, viability labeling was shown using three different labels (i.e. GFP, SYTO9/PI, and CDs). Finally, versatility in terms of fluorescent microscopy was demonstrated, serving as inspiration to further considering smartphone based fluorescent imaging with appropriate fluorescent tags. Other future perspectives include the used of other bioreceptors (e.g. lectins, antibodies, phages, or peptides) to isolate other target cells.

Acknowledgements

Authors would like to thank staff from the University of Florida (UF) Nanoscale Research Facility, the UF Interdisciplinary Center for Biotechnology Research, EnCor Biotechnology, Inc., and Dr. Carlos Rinaldi for assistance with the research. This work is supported by the US Army Medical Research and Materiel Command under SBIR Contract No. W81XWH-17-C-0109 led by Innovative Space Technologies, LLC and also by the USDA National Institute of Food and Agriculture, AFRI project No. 2017-08795. The views, opinions, and/or findings contained in this report are those of the author(s) and should not be construed as an official Department of the Army position, policy or decision unless so designated by other documentation.

Appendix A. Supplementary data

Supplementary material related to this article can be found, in the online version, at doi:https://doi.org/10.1016/j.snb.2019.04.043.

References

[1] World Health Organization, Food Safety [WWW Document], (2017) URL (Accessed 12 March 2018) http://www.who.int/news-room/fact-sheets/detail/food-safety.
[2] World Health Organization, Drinking-water [WWW Document], (2017) URL (Accessed 12 March 2018) http://www.who.int/news-room/fact-sheets/detail/drinking-water.
[3] World Health Organization, Guidelines for Drinking-water Quality First Addendum to Third Edition Volume 1 Recommendations, (2006).
[4] D.W. Meals, S.A. Dressing, T.E. Davenport, Lag time in water quality response to best management practices: a review, J. Environ. Qual. 39 (2010) 85, https://doi.org/10.2134/jeq2009.0108.
[5] A. Rasekh, A. Hassanzadeh, S. Mulchandani, S. Modi, M.K. Banks, Smart water networks and cyber security, J. Water Resour. Plan. Manag. 142 (2016) 01816004, , https://doi.org/10.1061/(ASCE)WR.1943-5452.0000646.
[6] M. Amiri, A. Bezaatpour, H. Jafari, R. Boukherroub, S. Szunerits, Electrochemical Methodologies for the Detection of Pathogens, (2018), https://doi.org/10.1021/acssensors.8b00239.
[7] D.C. Vanegas, C.L. Gomes, N.D. Cavallaro, D. Giraldo-Escobar, E.S. McLamore, Emerging Biorecognition and Transduction Schemes for Rapid Detection of Pathogenic Bacteria in Food, Compr. Rev. Food Sci. Food Saf. 16 (2017) 1188–1205, https://doi.org/10.1111/1541-4337.12294.
[8] B. Nasseri, N. Soleimani, N. Rabiee, A. Kalbasi, M. Karimi, M.R. Hamblin, Point-of-care microfluidic devices for pathogen detection, Biosens. Bioelectron. 117 (2018) 112–128, https://doi.org/10.1016/j.bios.2018.05.050.
[9] Q.A. Pankhurst, T.K. Thanh, S.K. Jones, J. Dobson, Progress in applications of magnetic nanoparticles in biomedicine, J. Phys. D Appl. Phys. 42 (2009) 15, https://doi.org/10.1088/0022-3727/42/22/224001.
[10] Q.A. Pankhurst, J. Connolly, S.K. Jones, J. Dobson, Applications of magnetic nanoparticles in biomedicine, J. Phys. D Appl. Phys. 36 (2003) 167–181.
[11] I. Šafařík, M. Šafaříková, Invited review magnetic nanoparticles and biosciences, Monatshefte fu Èr Chemie. (2002).
[12] V. Novosad, E. Rozhkova, Ferromagnets-based multifunctional nanoplatform for targeted cancer therapy, Biomedical Engineering, Trends in Materials Science, InTech, 2011, https://doi.org/10.5772/12928.
[13] M. Hofmann-Amtenbrink, B. Von Rechenberg, H. Hofmann, Chapter 5: Superparamagnetic nanoparticles for biomedical applications, Transworld Research Network, (2009).
[14] C.P. Hunt, B.M. Moskowitz, S.K. Banerjee, Magnetic properties of rocks and minerals, Am. Geophys. Union. (1995), https://doi.org/10.1029/RF003p0189.
[15] W. Jiang, K.-L. Lai, H. Hu, X.-B. Zeng, F. Lan, K.-X. Liu, Y. Wu, Z.-W. Gu, The effect of [Fe 3+]/[Fe 2+] molar ratio and iron salts concentration on the properties of superparamagnetic iron oxide nanoparticles in the water/ethanol/toluene system, J. Nanopart. Res. 13 (2011) 5135–5145, https://doi.org/10.1007/s11051-011-0495-8.
[16] A.S. Teja, P.-Y. Koh, Synthesis, properties, and applications of magnetic iron oxide nanoparticles, Prog. Cryst. Growth Charact. Mater. 55 (2009) 22–45, https://doi.org/10.1016/j.pcrysgrow.2008.08.003.

[17] V. Sundaresan, J.U. Menon, M. Rahimi, K.T. Nguyen, A.S. Wadajkar, Dual-responsive polymer-coated iron oxide nanoparticles for drug delivery and imaging applications, J. Pharm. 466 (2014) 1–7, https://doi.org/10.1016/j.ijpharm.2014.03.016.
[18] E.C. Alocilja, P. Jain, K. Pryg, Immunosensor for rapid extraction/detection of enteric pathogens, Technology 04 (2016) 194–200, https://doi.org/10.1142/S2339547816500072.
[19] D. Kwon, S. Lee, M. Mo Ahn, I.S. Kang, K.-H. Park, S. Jeon, Colorimetric detection of pathogenic bacteria using platinum-coated magnetic nanoparticle clusters and magnetophoretic chromatography, Anal. Chim. Acta 883 (2015) 61–66, https://doi.org/10.1016/j.aca.2015.04.044.
[20] M. Varshney, Y. Li, Interdigitated array microelectrode based impedance biosensor coupled with magnetic nanoparticle-antibody conjugates for detection of *Escherichia coli*O157:H7 in food samples, Biosens. Bioelectron. 22 (2007) 2408–2414, https://doi.org/10.1016/j.bios.2006.08.030.
[21] Y. Wang, E.C. Alocilja, Gold nanoparticle-labeled biosensor for rapid and sensitive detection of bacterial pathogens, J. Biol. Eng. 9 (2015), https://doi.org/10.1186/s13036-015-0014-z.
[22] R.P. Cowburn, D.K. Koltsov, A.O. Adeyeye, M.E. Welland, D.M. Tricker, Single-Domain Circular Nanomagnets, (1999).
[23] W. Scholz, K.Y. Guslienko, V. Novosad, D. Suess, T. Schrefl, R.W. Chantrell, J. Fidler, Transition from single-domain to vortex state in soft magnetic cylindrical nanodots, J. Magn. Magn. Mater. 266 (2003) 155–163, https://doi.org/10.1016/S0304-8853(03)00466-9.
[24] D.-H. Kim, E.A. Rozhkova, I.V. Ulasov, S.D. Bader, T. Rajh, M.S. Lesniak, V. Novosad, Biofunctionalized magnetic-vortex microdiscs for targeted cancer-cell destruction, Nat. Mater. 9 (2009), https://doi.org/10.1038/NMAT2591.
[25] N. Garraud, D.P. Arnold, Characterization of fluids via measurement of the rotational dynamics of suspended magnetic microdiscs, Crit. J. Appl. Phys. 117 (2015) 17–320, https://doi.org/10.1063/1.4918784.
[26] K.Y. Castillo-Torres, N. Garraud, D.P. Arnold, E.S. McLamore, Towards Pathogen Detection Via Optical Interrogation of Magnetic Microdiscs. Tech. Dig. Solid-state Sensors, Actuators, Microsystems Work. (hilt. Head 2016), (2016).
[27] K.Y. Castillo-Torres, N. Garraud, D.P. Arnold, E.S. McLamore, B.M. Cullum, D. Kiehl, E.S. McLamore (Eds.), Investigation of Magnetic Microdiscs for Bacterial Pathogen Detection, International Society for Optics and Photonics, 2016, , https://doi.org/10.1117/12.2228610 p. 98630G.
[28] X. Liu, J. Pang, F. Xu, X. Zhang, Simple approach to synthesize amino-functionalized carbon dots by carbonization of chitosan, Sci. Rep. 6 (2016) 31100, https://doi.org/10.1038/srep31100.
[29] S. Marton, F. Cleto, M.A. Krieger, J. Cardoso, Isolation of an aptamer that binds specifically to *E. Coli*, PLoS One 11 (2016) e0153637, , https://doi.org/10.1371/journal.pone.0153637.
[30] S.L. Burrs, M. Bhargava, R. Sidhu, J. Kiernan-Lewis, C. Gomes, J.C. Claussen, E.S. Mclamore, A paper based graphene-nanocauliflower hybrid composite for point of care biosensing, Biosens. Bioelectron. 85 (2016) 479–487, https://doi.org/10.1016/j.bios.2016.05.037.
[31] Y. Rong, A.V. Padron, K.J. Hagerty, N. Nelson, S. Chi, N.O. Keyhani, J. Katz, S.P.A. Datta, C. Gomes, E.S. Mclamore, Post hoc support vector machine learning for impedimetric biosensors based on weak protein-ligand interactions †, Analyst 143 (2018), https://doi.org/10.1039/c8an00065d.
[32] Y.-P. Sun, B. Zhou, Y. Lin, W. Wang, K.A.S. Fernando, P. Pathak, M.J. Meziani, B.A. Harruff, X. Wang, H. Wang, P.G. Luo, H. Yang, M.E. Kose, B. Chen, L.M. Veca, S.-Y. Xie, Quantum-sized carbon dots for bright and colorful photoluminescence, J. Am. Chem. Soc. 128 (2006) 7756–7757, https://doi.org/10.1021/ja062677d.
[33] O.J. Achadu, T. Nyokong, Application of graphene quantum dots decorated with TEMPO-derivatized zinc phthalocyanine as novel nanoprobes: probing the sensitive detection of ascorbic acid, New J. Chem. 40 (2016) 8727, https://doi.org/10.1039/c6nj01796g.
[34] X.-W. Hua, Y.-W. Bao, H.-Y. Wang, Z. Chen, F.-G. Wu, Bacteria-derived fluorescent carbon dots for microbial live/dead differentiation †, Nanoscale 9 (2017) 2150, https://doi.org/10.1039/c6nr06558a.
[35] S. Ying Lim, W. Shen, Z. Gao, Carbon quantum dots and their applications, This J. is Cite this Chem. Soc. Rev 44 (2015) 362, https://doi.org/10.1039/c4cs00269e.
[36] K.D. Hills, D.A. Oliveira, N.D. Cavallaro, C.L. Gomes, E.S. Mclamore, Actuation of chitosan-aptamer nanobrush borders for pathogen sensing †, Analyst 143 (2018) 1650, https://doi.org/10.1039/c7an02039b.
[37] P. Stiefel, S. Schmidt-Emrich, K. Maniura-Weber, Q. Ren, Critical aspects of using bacterial cell viability assays with the fluorophores SYTO9 and propidium iodide, BMC Microbiol. 15 (2015) 36, https://doi.org/10.1186/s12866-015-0376-x.
[38] U.S. Environmental Protection Agency, Revised Total Coliform Rule (RTCR): A Quick Reference Guide, (2013).
[39] P. Schmid-Hempel, S.A. Frank, Pathogenesis, Virulence, and Infective Dose, (2007), https://doi.org/10.1371/journal.ppat.0030147.
[40] A.H. Havelaar, K.M. Vazquez, Z. Topalcengiz, R. Muñoz-Carpena, M.D. Danyluk, Evaluating the U.S. Food safety modernization act produce safety rule standard for microbial quality of agricultural water for growing produce, J. Food Prot. 80 (2017) 1832–1841, https://doi.org/10.4315/0362-028X.JFP-17-122.
[41] E.B. Setterington, E.C. Alocilja, Electrochemical biosensor for rapid and sensitive detection of magnetically extracted bacterial pathogens, Biosensors 2 (2012) 15–31, https://doi.org/10.3390/bios2010015.
[42] H. Jayamohan, B. Gale, B. Minson, C. Lambert, N. Gordon, H. Sant, H. Jayamohan, B.K. Gale, B. Minson, C.J. Lambert, N. Gordon, H.J. Sant, Highly sensitive bacteria quantification using immunomagnetic separation and electrochemical detection of guanine-labeled secondary beads, Sensors 15 (2015) 12034–12052, https://doi.org/10.3390/s150512034.
[43] Y. Jin, J. Deng, J. Liang, C. Shan, M. Tong, Efficient bacteria capture and inactivation by cetyltrimethylammonium bromide modified magnetic nanoparticles, Colloids Surf. B Biointerfaces 136 (2015) 659–665, https://doi.org/10.1016/j.colsurfb.2015.10.009.
[44] S. Zhan, D. Zhu, S. Ma, W. Yu, Y. Jia, Y. Li, H. Yu, Z. Shen, Highly Efficient Removal of Pathogenic Bacteria with Magnetic Graphene Composite, (2015), https://doi.org/10.1021/am508682s.
[45] Y. Luo, E.C. Alocilja, Portable nuclear magnetic resonance biosensor and assay for a highly sensitive and rapid detection of foodborne bacteria in complex matrices, J. Biol. Eng. 11 (2017) 14, https://doi.org/10.1186/s13036-017-0053-8.
[46] R.A. Bohara, N.D. Throat, N.A. Mulla, S.H. Pawar, Surface-Modified Cobalt Ferrite Nanoparticles for Rapid Capture, Detection, and Removal of Pathogens: a Potential Material for Water Purification, Appl. Biochem. Biotechnol. 182 (2017) 598–608, https://doi.org/10.1007/s12010-016-2347-6.
[47] F. Halouane, R. Jijie, D. Meziane, C. Li, S.K. Singh, J. Bouckaert, J. Jurazek, S. Kurungot, A. Barras, M. Li, R. Boukherroub, S. Szunerits, Selective isolation and eradication of *E. coli* associated with urinary tract infections using anti-fimbrial modified magnetic reduced graphene oxide nanoheaters †, J. Mater. Chem. B 5 (2017) 8133, https://doi.org/10.1039/c7tb01890h.
[48] Y. Xu, H. Wang, C. Luan, Y. Liu, B. Chen, Y. Zhao, Aptamer-based hydrogel barcodes for the capture and detection of multiple types of pathogenic bacteria, Biosens. Bioelectron. 100 (2018) 404–410, https://doi.org/10.1016/j.bios.2017.09.032.
[49] H.C. Koydemir, Z. Gorocs, D. Tseng, B. Cortazar, S. Feng, R.Y.L. Chan, J. Burbano, E. McLeod, A. Ozcan, Rapid imaging, detection and quantification of Giardia lamblia cysts using mobile-phone based fluorescent microscopy and machine learning, Lab Chip 15 (2015) 1284–1293, https://doi.org/10.1039/C4LC01358A.
[50] P. Han, D. Dong, X. Zhao, L. Jiao, Y. Lang, A smartphone-based soil color sensor: for soil type classification, Comput. Electron. Agric. 123 (2016) 232–241, https://doi.org/10.1016/J.COMPAG.2016.02.024.

Graduate Research Assistant – Mrs. Keisha Castillo-Torres Keisha Y. Castillo-Torres is a graduate (PhD) research assistant within the Interdisciplinary Microsystems Group (IMG) and the Electrical and Computer Engineering department at the University of Florida. Keisha obtained her B.S. degree (2015) in electrical engineering at the University of Puerto Rico at Mayagüez. She is working under the co-advisement of Dr. Arnold and Dr. McLamore on the application of magnetic microdiscs for detection of waterborne and foodborne bacterial pathogens. Keisha is a Student Member of the IEEE (IEEE Young Professionals, IEEE Women in Engineering, and IEEE Engineering in Medicine and Biology Society) and a member of Tau Beta Pi.

Professor – Dr. David Arnold David P. Arnold is the George Kirkland Engineering Leadership Professor in the Department of Electrical and Computer Engineering, Deputy Director of the NSF Multi-functional Integrated System Technology (MIST) Center, and Director of the Interdisciplinary Microsystems Group at the University of Florida. He received dual B.S. (1999) and M.S. degrees (2001) from University of Florida and the Ph.D. degree in electrical and computer engineering from Georgia Tech (2004). His research focuses on micro/nanostructured magnetic materials, magnetic microsystems, electromechanical transducers, and miniaturized power/energy systems. He is an active participant in the magnetics and MEMS communities and serves on the editorial boards of J. Micromechanics and Microengineering and Energy Harvesting and Systems. He has co-authored over 170 refereed journal and conference publications and holds 17 U.S. patents. His research innovations have been recognized by the 2008 Presidential Early Career Award in Science and Engineering (PECASE) and the 2009 DARPA Young Faculty Award.

Professor – Dr. Eric McLamore Eric S. McLamore is an Associate Professor in Agricultural and Biological Engineering at the University of Florida. He earned his Ph.D. in Civil/Ag & Bioengineering from Purdue University in 2008. His background is in biological/environmental engineering and instrumentation, and his interests are in low cost biosensors for agricultural, environmental, and biomedical applications. He has been awarded numerous research and education awards, including the USDA New Teacher Award for Excellence in Teaching in the Food and Agricultural Sciences (2016), the American Society of Agricultural and Biological Engineering (ASABE) A.W. Farrall Young Educator Award (2015), and the ASABE Florida Section Teacher of the Year (2014). He has co-authored 84 peer reviewed journal articles (excluding conference proceedings), and 4 book chapters. He is a Fulbright research scholar and project leader of three international projects related to humanitarian efforts in Colombia and Cambodia for providing safe water/food to vulnerable communities. Dr. McLamore is also a member of the UF Water Institute.